Magnetic field measurement based on a stimulated two-photon Raman transition*

Zhou Zi-Chao(周子超), Wei Rong(魏 荣)†, Shi Chun-Yan(史春艳), Li Tang(李 唐), and Wang Yu-Zhu(王育竹)†

Key Laboratory of Quantum Optics, Shanghai Institute of Optics and Fine Mechanics, Chinese Academy of Sciences, Shanghai 201800, *China*

(Received 12 June 2010; revised manuscript received 15 July 2010)

The magnetic field in the microwave interaction zone of the fountain atomic clock was measured by stimulated Raman transitions. By measuring the two-photon transition frequency between the Zeeman levels of the two ground states, we achieved a magnetic field measurement accuracy of the order of 0.28 nT. This method is immune to the Doppler shift and the AC Stark shift. The second order Zeeman shift of the fountain clock is 170.7×10^{-15}, with the uncertainty of 7.2×10^{-16}.

Keywords: fountain atomic clock, Raman transition, second order Zeeman shift

PACS: 42.65.Dr, 95.55.Sh **DOI:** 10.1088/1674-1056/20/3/034206

The development of laser cooling and trapping techniques has opened the door to a radical approach in the construction of atomic clocks.[1,2] The atomic fountain clock is the most accurate microwave clock that currently contributes to International Atomic Time. Recently, the frequency stability and uncertainty of the atomic fountain clock has reached the 10^{-16} level.[3] The uncertainty of the atomic fountain clock is not evaluated by comparing it with other frequency standards, such as statistical (type-A) uncertainty, but by analysing all known systematic (type-B) uncertainties of the clock transition. In the accuracy budget of all shifts, the three most important effects have been identified as the second-order Zeeman Effect, blackbody radiation and collisions.[4−8] For the evaluation of the second-order Zeeman effect, one must depict the whole magnetic field in the interaction zone. The whole magnetic field map is normally attained by measuring the frequency of magnetically sensitive transitions with microwave or low radio frequency.[9]

The rubidium fountain clock was constructed at the Shanghai Institute of Optics and Fine Mechanics in 2005,[10] the Ramsey fringe with high signal-to-noise ratio was acquired in 2009.[11] Recently, the type-B uncertainty of the device has been evaluated. Magnetic field mapping has been the subject of an increasing number of important works in recent years. Normal ways of mapping include the radio frequency method, which detects low-frequency transitions of magnetic sublevels of the same hyperfine state,[9] and the microwave radiating method, which detects microwave transitions of magnetic sublevels of different hyperfine states.[10] The former requires additional coils and may bring about magnetic noise in measuring, while the latter is simpler and is utilized in the same device we have used.[11] However, the latter method cannot map a whole microwave interaction zone and cannot be seeded to a certain position, such as a cut-off waveguide. The method based on two-photon stimulated Raman transitions is used to map the C-field in this letter. The proposed method does not bring about additional noise to the fountain and can map the whole interaction zone of the fountain.

The principle of the method is as follows. The atoms are stimulated and transitioned between the Zeeman sublevels of the ground states using the interaction with the Raman pulse of two copropagating beams. In this process, these transitions become sensitive to the Doppler shift and the ac Stark shift. Nevertheless, the frequency difference between the neighbouring Raman transitions, which is proportional to the magnetic field intensity, is unaffected by these shifts.

The stimulated Raman transition has been widely used in the field of atom interferometry.[12−14] In

*Project supported by the National Basic Research Program of China (Grant No. 2005CB724506), the National Natural Science Foundation of China (Grant Nos. 10604058 and 10974215), and by the Open Research Fund of State Key Laboratory of Precision Spectroscope.

†Corresponding author. E-mail: weirong@siom.ac.cn yzwang@mail.shcnc.ac.cn

© 2011 Chinese Physical Society and IOP Publishing Ltd

the theoretical analysis of the stimulated Raman transition,[14,15] the transition probability can be described as:

$$P_{\rm a} = \frac{2\Omega_{\rm eff}^2}{\left(\delta^{\rm AC}-\delta\right)^2+4\Omega_{\rm eff}^2} \times\left(1-\cos\left(\sqrt{\left(\delta^{\rm AC}-\delta\right)^2+4\Omega_{\rm eff}^2}\tau\right)\right). \quad (1)$$

The energy structure of the stimulated Raman transition is depicted in Fig. 1. In this equation, $\Omega_{\rm eff} = \Omega_1^*\Omega_2/4\Delta$, $\delta^{\rm AC} = \Omega_{\rm a}^{\rm AC} - \Omega_{\rm b}^{\rm AC}$, $\Omega_{\rm a}^{\rm AC} = \Omega_1^2/4\Delta$, and $\Omega_{\rm b}^{\rm AC} = \Omega_2^2/4\Delta$. In addition, $|a\rangle, |b\rangle$ are the two ground states, Ω_i is the Rabi frequency used to characterize the level coupling by the ith ($i = 1, 2$) laser beam, $\Omega_{\rm eff}$ is the effective Rabi frequency of the two-photon transition, δ is the detuning from the Raman resonance in the absence of AC Stark shift, and $\delta^{\rm AC}$ is the whole AC Stark shift of two ground states. In addition, $\Omega_{\rm a}^{\rm AC}$ and $\Omega_{\rm b}^{\rm AC}$ are the ac Stark shifts of level $|a\rangle$ and level $|b\rangle$, respectively, τ is the Raman pulse width, and Δ is the Raman beam detuning from the excited state. This equation could be obtained when the detuning from the excited states are larger than the Rabi frequencies, $\Delta >> \Omega$. In the scheme that we used, the two Raman beams were copropagating, thus the influence of the photon momentum was neglected. However, the different Doppler shifts of the two beams influenced the central transition frequency.

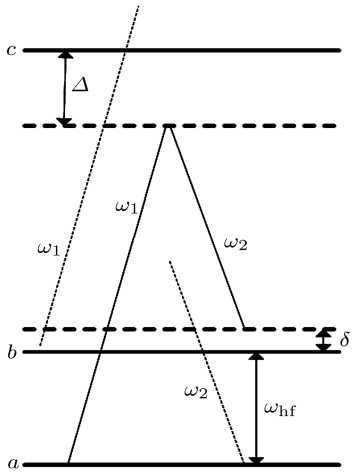


Fig. 1. Energy level of the two-photon stimulated Raman transition. The case of the two Raman beams (ω_1, ω_2) in dash line was not considered when the AC Stark shift of the two ground states was calculated.

In this experiment, about 10^8 ^{87}Rb atoms in the upper state $F = 2$ were collected in the magnetic–optic trap in 500 ms and further cooled in optical molasses to about 4 μK. The atoms then underwent post cooling and were launched vertically in (1, 1, 1) geometry by moving optical molasses with an initial velocity of about 4 m/s in a few milliseconds. The upward going atoms entered the interaction zone, which was magnetically attenuated by four layers of mu-metal shield. A highly homogeneous 150 nT static magnetic field (about 150 nT) was produced by a solenoid and compensation coils surrounding the microwave and free-flight region. The environment magnetic field was attenuated by 40 dB, and the residual magnetic field fluctuation was expected to be less than 2 nT. The time of flight signals were obtained at the detection zone using two probe beams.

The Raman beams were generated by fibre electric–optic modulator (FEOM) driven by the signal generator referred to as the Hydrogen maser. The input laser beam was provided by the diode laser, which was locked to the crossover peak of $F = 2 \rightarrow F' = 2$ and $F = 2 \rightarrow F' = 3$ of D2 line of ^{87}Rb. Prior to coupling it to the FEOM, the laser beam was shifted by a double-pass optical path of a 200 MHz acoustic–optic modulator that was also used to switch off the Raman beam. The FEOM driver frequency was swept around 6.835 GHz to stimulate the Raman transitions between the magnetic levels of the ground states. Its carrier and the +1th sideband were used as the two Raman beams. The residual sidebands of the FEOM can be neglected for their far detuning. The ratio of the two components can be changed by sweeping the driver power of the FEOM. The output beams were then delivered to the fountain physics system through polarization maintaining fibre. The final beams that have parallel linear polarizations have a total power of 0.04 mW in 1.4 cm Gaussian diametre. The effective Rabi frequency of the Raman transition was about 550 Hz.

The magnetic intensity of the point of interaction zone was detected through the following ways: when atoms pass by the point, a 12 ms pulse of Raman beams was switched on, facilitating their interaction with the atoms. The Raman transitions can be shown by measuring the variation of transition probability following the modulation frequency of the FEOM (Fig. 2). The magnetic intensity of the location of the atoms was obtained by calculating the distances of the peaks. The whole magnetic field map was acquired when the time delay of Raman pulse was swept step by step. As pointed out in an earlier study,[16] the σ transition is forbidden given that the propagation direction of the Raman beams is parallel

to the vertical C-field. The width of the transition is mainly limited by the Raman pulse width.

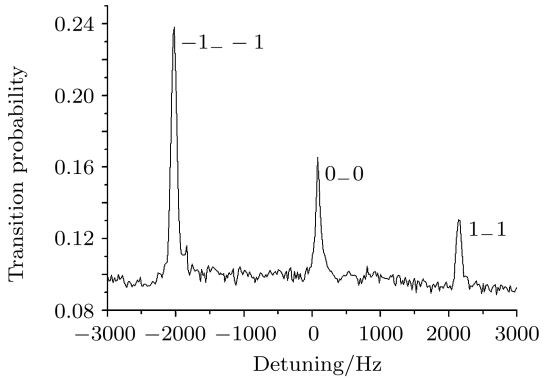


Fig. 2. Resonance curve of the stimulated two-photon Raman transition probability following frequency detuning δ of Raman beams; here, the Raman pulse is switched on for 12 ms after 425 ms from the time the atoms are launched. The driver power of EOM is 10 dbm, and the frequency step is 10 Hz. The $\Delta m_{\rm F} \neq 0$ transitions are forbidden.

In Fig. 2, the central frequency of the Raman transition is offset from the clock frequency. This offset was mainly caused by the Doppler shift and AC Stark shift of the Raman beams. For the copropagating Raman beams, the Doppler shift of the atoms with velocity ν can be expressed as:

$$\upsilon = -(k_2 - k_1)\nu = \frac{\upsilon_{\rm hfs}}{c}\nu. \tag{2}$$

The variant frequency shift with time can be expressed as:

$$\frac{\delta\upsilon}{\delta t} = \frac{\upsilon_{\rm hfs}}{c}g. \tag{3}$$

In these equations, υ is the Doppler shift, $\upsilon_{\rm hfs} = 6.83468\cdots$ GHz is the ^{87}Rb hyperfine structure splitting of the ground state, c is the light speed, and g is the gravity acceleration. The relationship between the time delay of the Raman pulse and the central frequency of 0–0 transition is depicted in Fig. 3. We attained the gradient of the frequency shift through the linear fitting of the data. The resulting experiment gradient is about 0.251 Hz/ms, which is near the theoretical value of 0.223 Hz/ms within 12% error.

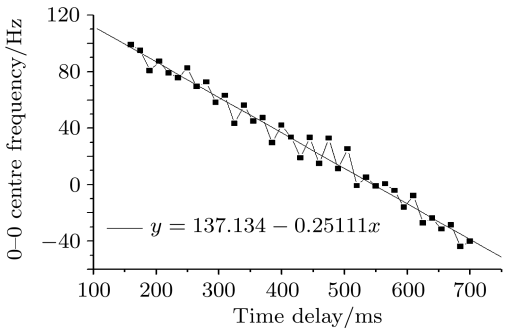


Fig. 3. Centre frequency of 0–0 transition versus the delay time of the Raman pulse. The origin point of the x axis is the time of launching the cold atoms. Error of the gradient between the experimental result and the theoretical calculation is within 12%.

The AC Stark shift of the ground states also caused the offset of the resonant frequency of Raman transitions. Although the two Raman beams shifted both ground states, we only considered the detuning Δ, which is smaller than the splitting of the ground states. The Stark shift of the two Raman beams (dashed line in Fig. 1) is neglected. In the present experiment, the detuning Δ is about 127 MHz. Normally, $\Omega_{\rm a}^{\rm AC}$ and $\Omega_{\rm b}^{\rm AC}$, the AC Stark shifts of the two transitions are around 100 Hz. When the intensities of the two Raman beams are equal, $\delta^{\rm AC}$ (the total AC Stark shift of Raman transitions) becomes zero. This can be realized by tuning the driver power of EOM. The relationship between the AC Stark shift and relative power of two laser beams are depicted in Fig. 4.

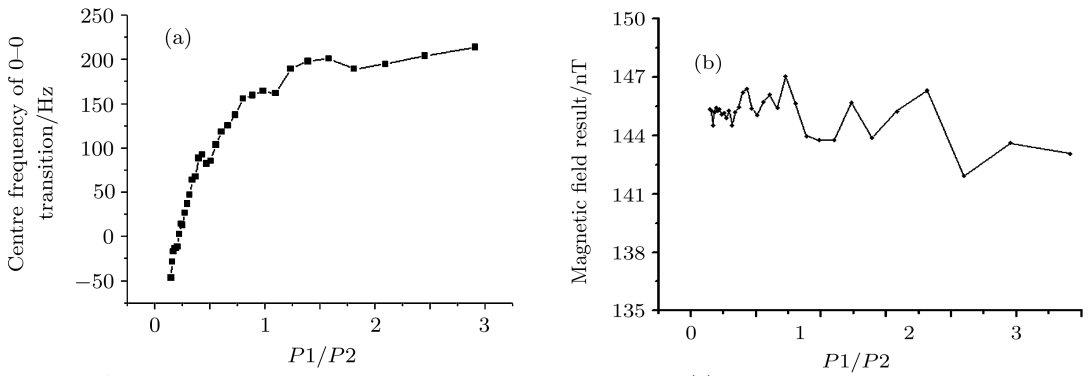


Fig. 4. The AC Stark shift versus the driver power of the EOM. In Fig. 4(a), the centre frequency of 0–0 transition is changed with the driver power since the total ac Stark shift is varied for the different ratio of the two Raman beams. Figure 4(b) depicts the measurement results calculated from the difference frequency of neighbouring transition versus the power ratio of the two Raman beams. The influence of the AC Stark shift can be neglected for the magnetic field measurement. The data is attained at the 350 ms point.

The offset caused by the Doppler shift and AC Stark shift is equal to the neighbouring transition. Thus, this offset is not considered an obstacle to the magnetic field measurement. The fluctuation of the measured magnetic field in Fig. 4(b) is mainly caused by the error of fitting the Raman transitions. When the ratio between the two Raman beams is larger than 1, the total power is decreased drastically and the signal to noise ratio of the Raman transitions is lower, which brings about the error in the measurement. But this fluctuation is much lower than the AC Stark shift.

The magnetic intensity is measured by calculating the difference of Raman transition peaks. The magnetic field map of the interaction zone is depicted in Fig. 5. The central transition frequency between the magnetic levels was identified within 2 Hz, which corresponded to 0.28 nT. Typically, the measurement of the magnetic field has a 0.4% relative uncertainty. To verify the method, an additional experiment was performed through the mapping magnetic intensity with microwave radiation, which was based on our previous work.[17] The error between the measurement results was less than 1 nT (Fig. 5).

The second order Zeeman shift of the clock transition can be directly evaluated by calculating the time average of the square of the magnetic field. The coefficient of the second order Zeeman shift of ^{87}Rb is $\delta v = 575.15\ \mathrm{Hz/G^2} \times \langle B^2(t)\rangle$. We used $\langle B(t)\rangle^2$ instead of $\langle B^2(t)\rangle$ in the whole trajectory above the Ramsey cavity. This shift of the ^{87}Rb fountain clock was evaluated as 1.17 mHz, and the bias of the second order Zeeman shift was 170.7×10^{-15}. The uncertainty of this shift was about 7.2×10^{-16}.

In conclusion, we have measured the magnetic intensity map of interaction zone of the ^{87}Rb fountain atomic clock through the stimulated two-photon Raman transition. By sweeping the driver frequency of the EOM, we observed the $\Delta m_{\mathrm{F}} = 0$ transitions between the Zeeman levels of the ground states. The centre of the resonance for the Doppler shift and AC Stark shift of the Raman pulse shifts. However, the difference of the neighbouring transitions is immune to these shifts. In addition, the whole magnetic field map in the interaction zone was depicted by sweeping time delay of the Raman pulse. The magnetic field is not as homogenous compared with the design of this experiment. In future works, the homogeneity should be improved toward precise compensation of the fluctuation of the magnetic field.

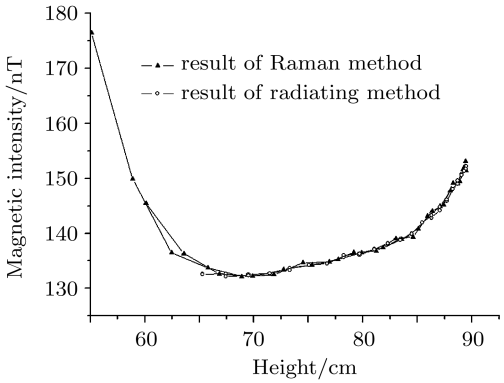


Fig. 5. Map of the magnetic field in and above the Ramsey cavity. The origin of the x axis is the center of the magnetic–optic trap. The first point of the map is the location of the Ramsey cavity. The C-field at the Ramsey cavity is distorted by the residual magnetic field of the components of the cavity. The uncertainty of the data (0.4%) is smaller than the symbol. The black triangle lineshape of magnetic field is the result of Raman method which the blank circle is the result of radiating method.

Acknowledgments

We are grateful for the discussion with Professor Xu Xin-Ye at East China Normal University.

References

[1] Vian C, Rosenbunch P, Marion H, Bize S, Cacciapuoti L, Zhang S, Abgrall M, Chambon D, Maksimovic I, Laurent P, Santarelli G, Clairon A, Luiten A, Tobar M and Salomon C 2005 *IEEE Instrum. Meas.* **54** 833

[2] Ludlow A D, Zelevinsky T, Campbell G K, Blatt S, Boyd M M, de Miranda M H G, Martin M J, Thomsen J W, Foreman S M, Ye Jun, Fortier T M, Stalnaker J E, Diddams S A, Le Coq Y, Barber Z W, Poli N, Lemke N D, Beck K M and Oates C W 2008 *Science* **319** 1805

[3] Heavner T P, Jefferts S R, Donley E A, Shirley J H and Parker T E 2005 *IEEE Instrum. Meas.* **54** 842

[4] Wynands R and Weyers S 2005 *Metrologia.* **42** S64

[5] Itano W M, Lewis L L and Wineland D J 1982 *Phys. Rev.* A **25** 1233

[6] Levi F, Calonico D, Micalizio S and Godone A 2004 *Phys. Rev.* A **70** 033412

[7] Gibble K and Chu S 1993 *Phys. Rev. Lett.* **70** 1771

[8] Dos Santos F P, Marion H, Bize S, Sortais Y, Clairon A and Salomon C 2002 *Phys. Rev. Lett.* **89** 233004

[9] Jefferts S R, Shirley J, Parker T E, Heavner T P, Meekhof D M, Nelseon C, Levi F, Costanzo G, De Marchi A, Drullinger R, Hollberg L, Lee W D and Walls F L 2002 *Metrologia.* **39** 321

[10] Wei R, Qian Y, Zhang Y and Wang Y Z 2003 *Chin. Phys. Lett.* **21** 57
[11] Zhou Z, Wei R, Shi C, Lv D, Li T and Wang Y 2009 *Chin. Phys. Lett.* **26** 123201
[12] Weiss D S, Young B C and Chu S 1993 *Phys. Rev. Lett.* **70** 2706
[13] Ke M, Yan B, Cheng F and Wang Y 2009 *Chin. Phys.* B **18** 4824
[14] Weiss D S, Young B C and Chu S 1994 *Appl. Phys.* B **59** 217
[15] Moler K, Weiss D S, Kasevich M and Chu S 1992 *Phys. Rev.* A **45** 342
[16] Bonin K D and Mcllrath T 1984 *J. Opt. Soc. Am.* B **1** 52
[17] Shi C, Wei R, Zhou Z, Lv D, Li T and Wang Y 2010 *Chin. Opt. Lett.* **8** 549